Available online at www.sciencedirect.com
ScienceDirect
Solid-State Electronics 51 (2007) 64–68
SOLID-STATE ELECTRONICS
www.elsevier.com/locate/sse

Structure design criteria of dual-channel high mobility electron transistors

Jia-Chuan Lin [a,*], Yu-Chieh Chen [b], Wei-Chih Tsai [c], Po-Yu Yang [d]

[a] Department of Electronics Engineering, St. John's University, Taiwan, ROC
[b] Institute of Automation and Mechatronics, St. John's University, Taiwan, ROC
[c] Institute of Microelectronics, Department of Electrical Engineering, National Cheng Kung University, Taiwan, ROC
[d] Department of Photonics & Display Institute, National Chiao Tung University, Taiwan, ROC

Received 7 March 2006; received in revised form 17 October 2006; accepted 27 November 2006
Available online 16 January 2007

The review of this paper was arranged by Prof. Y. Arakawa

Abstract

The design criteria of dual-channel high electron mobility transistor (DHEMT) are proposed in this study. δ-Doped $In_{0.52}Al_{0.48}As$/$In_{0.53}Ga_{0.47}As$/InP material systems are concentrated in this article. The DHEMT structures are explored numerically and compared with conventional single-channel high electron mobility transistor (SHEMT) structures. Some criteria of doping concentration and layer structure design are proposed. The simulation results reveal that DHEMT has a larger voltage swing, a lower gate leakage current, a better carrier confinement, a higher density of two-dimensional electron gas (2DEG) and an excellent transconductance than SHEMT.

Keywords: Dual-channel; Single-channel; δ-Doping; HEMT; 2DEG

1. Introduction

InP/InGaAs high electron mobility transistors (HEMTs) have superior electronic transport properties to GaAs/AlGaAs HEMTs due to the large Gamma–L band separation, low effective mass, higher low-field electron mobility, high electron saturation velocity, and higher sheet carrier densities in the InGaAs channel [1–3]. However, the high electron affinity in the InGaAs channel layer may induce impact ionization field under high electric field that would lead to a high leakage current, and hence, degrade output conductance, voltage gain, and on-state breakdown voltage considerably [4].

Dual-channel structure based on modulation-doped GaAs/AlGaAs material system was first proposed in 1984 [5]. By the well controlling on the two-dimensional electron gas (2DEG), a larger output current and higher transconductance can be obtained in dual-channel high mobility electron transistors (DHEMTs) [6,7]. It attracted much attention for both analog and digital applications [1]. In this study, DHEMTs based on δ-doped $In_{0.52}Al_{0.48}As$/$In_{0.53}Ga_{0.47}As$/InP heterostructures are concentrated. It is investigated numerically and compared with conventional single-channel high electron mobility transistor (SHEMT) structures. Some criteria of doping concentration and layer structure design are proposed. It reveals that the dual-channel structure could reduce leakage current remarkably and upgrade the device performance. The transconductance may go up to 1836 ms/mm.

2. Structure design and simulation

Two-dimensional device simulator, MEDICI, is used to solve the Poisson's equation and the electron/hole current

* Corresponding author. Tel.: +886 02 28013131x6130; fax: +886 02 28013142.
E-mail address: jclin@mail.sju.edu.tw (J.-C. Lin).

0038-1101/$ - see front matter © 2006 Elsevier Ltd. All rights reserved.
doi:10.1016/j.sse.2006.11.016

continuity equations. Boltzmann transport theory is also applied. The carrier densities and electronic band structures are calculated. The influences of δ-doping concentration and position, gate width, spacer thickness, etc. on the device performances are explored.

Fig. 1 shows the schematic cross-section of (a) SHEMT and (b) DHEMT. InGaAs cap layer (250 Å) doped with silicon at $3\times10^{17}\,cm^{-3}$ to provide good source/drain Ohmic contacts are shown. The well designed pinch-off voltage can be obtained by the optimization of the thickness and doping concentration in the InAlAs barrier layer. In Fig. 1a, the active layer is composed of an $In_{0.52}Al_{0.48}As$ undoped barrier layer (250 Å thick), the δ-doping concentrations are $1\times10^{18}\,cm^{-3}$ for top δ-doped layer, and $3\times10^{17}\,cm^{-3}$ for bottom δ-doped layer., an undoped spacer layer (50 Å thick) for reducing Coulomb scattering [8], and an $In_{0.53}Ga_{0.47}As$ undoped channel layer (50 Å thick). In addition, an undoped InP buffer layer (1000 Å thick) is placed on the bottom layer. In order to keep the strong sensitivity of the gate control on the channel, the spacer must be as thin as possible. Furthermore, compared to modulation-doped structures, δ-doped structures have several merits, such as (1) high 2DEG concentration, (2) high electron mobility, (3) large breakdown voltage, (4) more linear and higher transconductance, (5) high drain current capability, and (5) low leakage current [9,4]. On the other hand, Fig. 1b shows the layer structure with a duplicate of the active layer of which an InAlAs barrier layer (200 Å thick), an undoped spacer layer (50 Å thick) and a channel layer with thickness (50 Å) are composed. Moreover, the performance of the devices depends strongly on the structures of the recess configuration. A narrow recess leads to low gate–drain breakdown voltage, whereas a wide recess introduces a current limiter, especially at the source. Therefore an asymmetric recess configuration is needed. A wider recess at the drain side is used to improve breakdown voltage and to reduce feedback effect. A narrow recess at the source side leads to a low parasitic source resistance [10].

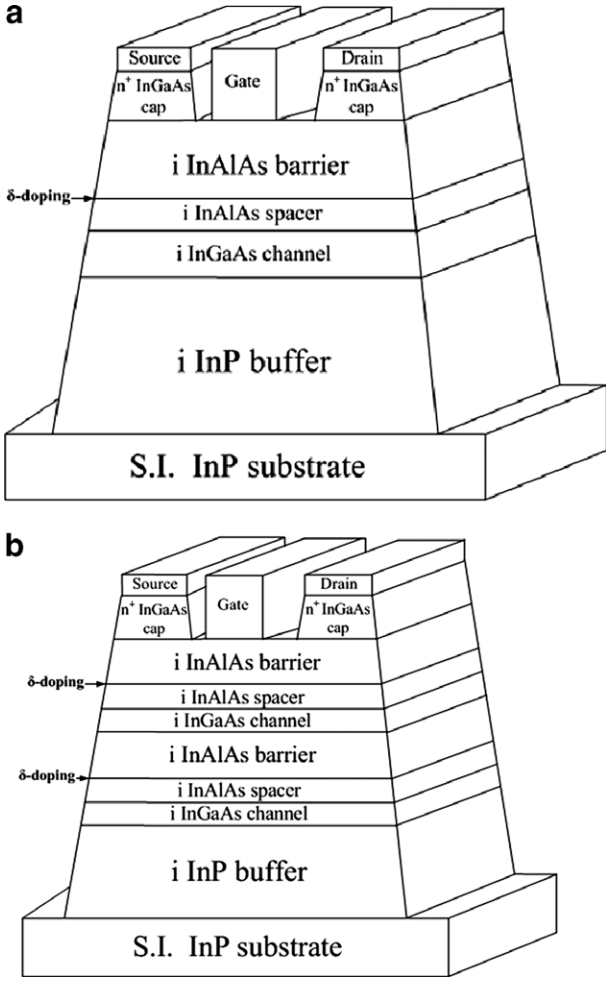

Fig. 1. Schematic cross-sections of the $In_{0.52}Al_{0.48}As/In_{0.53}Ga_{0.47}As/InP$ (a) SHEMT and (b) DHEMT.

The electron concentration distribution, n, may be calculated by solving the Poisson's and Schrödinger's equations self-consistently [11]. Poisson's equation is shown in Eq. (1) where n and p are the electron and hole concentrations, respectively.

$$\varepsilon\nabla^2\psi = -q(p-n+N_D^+-N_A^-)-\rho_S, \tag{1}$$

where N_D^+ and N_A^- are the ionized donor and acceptor concentrations, respectively, and ρ_s is a surface charge density. ψ is the electrostatic potential. For a HEMT structure, the threshold voltage V_T can be derived from Poisson's equation and is expressed as

$$V_T = \Phi_b - \frac{\Delta E_c}{q} - \frac{qN_d d_d}{\varepsilon_s}\left(d_c + \frac{d_d}{2}\right), \tag{2}$$

where Φ_b is the Schottky barrier height of the gate metal on the semiconductor; ΔE_c is the conduction band discontinuity between InGaP and InGaAs. N_d and d_d are the doping concentration and the thickness of the doped barrier layer, respectively. d_c is the thickness of the undoped barrier layer; and ε_s is the permittivity of the Schottky layer [12].

Conduction band electron tunneling effects are included in our simulation. The net tunneling current across the barrier layer is calculated using the independent electron approximation [13]

$$j_{DT} = \frac{4\pi q r_{DOS} m_1 k_{BT}}{h^3}\int_0^{E_b} T_C(E)\ln\left[\frac{e^{(E_{Fn1}-E_{c1}-E)/k_{BT}}+1}{e^{(E_{Fn3}-E_{c1}-E)/k_{BT}}+1}\right]dE, \tag{3}$$

where the integral is over the vertical kinetic energy, E, of the incident electrons. E_{Fn1}, E_{c1}, and m_1 are the electron quasi-Fermi level, the conduction band edge, and the electron effective tunneling mass, respectively, in the emitting layer. E_{Fn3} and E_{c3} are the corresponding electron quasi-Fermi level and conduction band edge in collecting layer. The electron charge is given by q, h is Planck's constant,

and k_{BT} is the thermal energy. T_C is the tunneling coefficient of an electron with energy E.

Tunneling through multiple barriers is evaluated numerically using the Airy Transmission Matrix Technique or AiryTMT [13,14]. Tunneling through the potential barrier is treated as a scattering problem. The tunneling coefficient is calculated as

$$T_C(E) = \frac{m_0}{m_{N+1}} \frac{k_{N+1}}{k_0} \frac{|T|^2}{|I|^2}, \quad (4)$$

where m_0 and m_{N+1} are the tunneling masses in the source and destination regions, respectively, and k_0 and k_{N+1} are the wave vectors of the carrier in the source and destination region, respectively.

3. Simulation results and discussions

Fig. 2 shows the energy band diagrams and the corresponding electron concentration distributions of (a) SHEMT and (b) DHEMT in thermal equilibrium. A channel layer that is near to the gate layer would keep a good sensitivity of gate control. On the other hand, a channel layer that is far from the gate layer would induce much more electrons in the channel because of the downward conduction band edge of the channel layer to the Fermi level from the Schottky barrier. Then, the design of dual-channel structure could come to a compromise between them. It is also clearly showed in Fig. 2 that the electron concentration of both two channels in DHEMT is much more than SHEMT. Fig. 3 shows the sheet carrier density (n_s) with gate bias of top and bottom channels of DHEMT, respectively. It shows that the top channel is more sensitive to the gate bias and exhibits a narrow range sheet carrier density distribution. In such a normally-on DHEMT, when a small negative bias is applied, the top channel turns off first. The bottom channel does not turn off until a large negative bias is applied. An excellent transconductance could be obtained when both of the two channels turn on. Fig. 4 shows the drain–source voltages (V_{DS}) versus drain–source current (I_{DS}) of (a) SHEMT and (b) DHEMT for various gate–source voltages (V_{GS}). DHEMT has a larger drain saturation current than SHEMT at the same gate bias and keeps a good pinch-off and breakdown voltage performance. In Fig. 5, V_{GS} versus I_{DS} and G_m of SHEMT and DHEMT are shown. DHEMT has a higher drain current up to 1425 mA/mm and a wider DC operation voltage 2.7 V (−1.4–1.3 V) than SHEMT. The G_m of DHEMT is up to 1836 mS/mm and higher than SHEMT. The result reaches the same conclusion as Fig. 2 that a deeper conduction band from Fermi level in DHEMT can lead to a higher electron concentration, a higher drain current and a higher G_m. The comparison of gate leakage current of SHEMT and DHEMT are shown in Fig. 6. The gate leakage current of DHEMT is much less than SHEMT, especially in large gate bias. To get a low leakage current in HEMT, some researchers take the InP channel instead of InGaAs channel [15,16]. However, it would reduce the carrier density in the channel and hence the G_m. A dual-channel structure would provide a good choice for it. Fig. 7 shows the variation of G_m under different top barrier thickness (T_1) and bottom barrier thickness (T_2) in DHEMTs. The maximum G_m can reach to 1836 mS/mm in most cases. However,

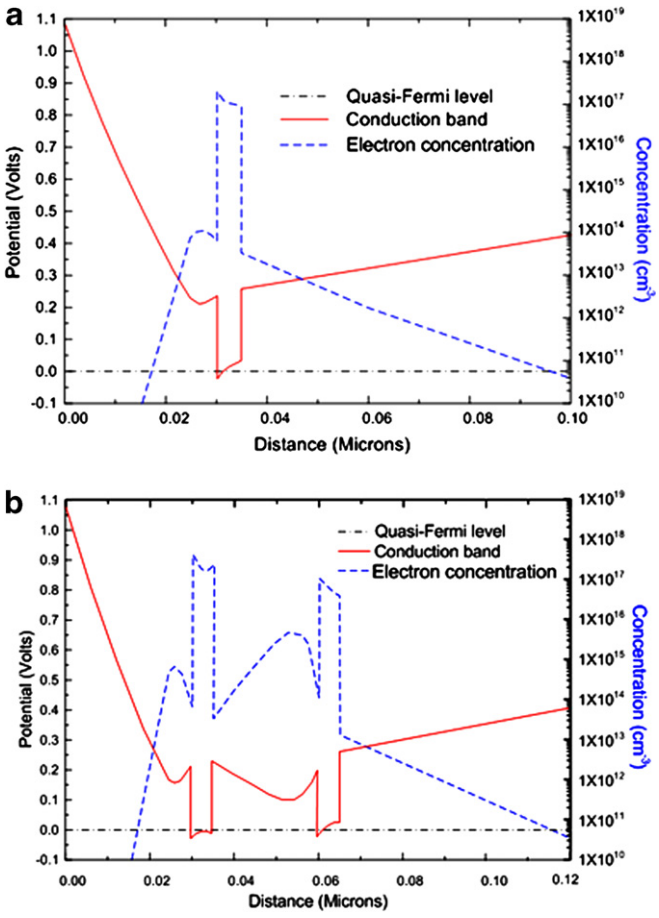

Fig. 2. Simulation conduction band and electron concentration distribution diagram of (a) SHEMT and (b) DHEMT in thermal equilibrium.

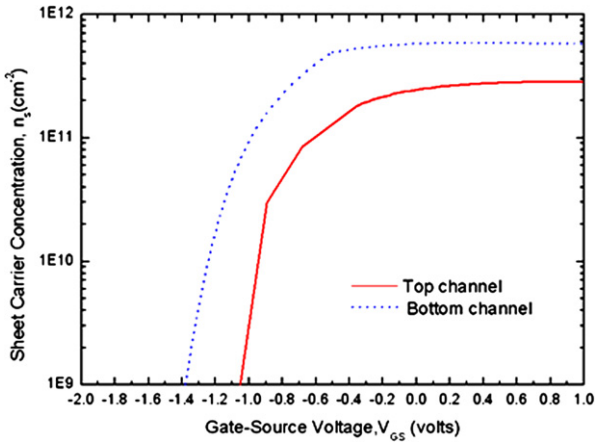

Fig. 3. The sheet carrier densities under various gate biases in top channel and bottom channel of DHEMT.

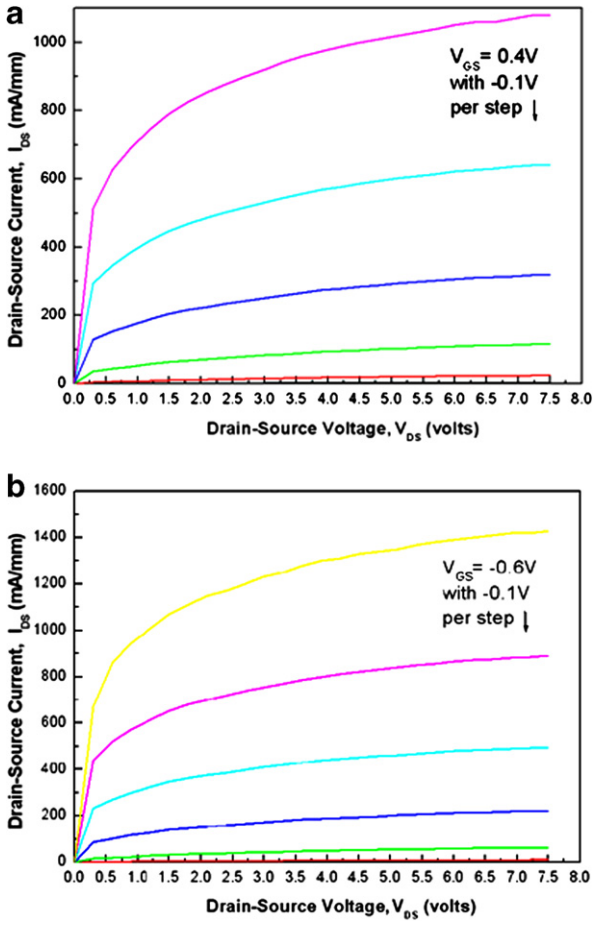

Fig. 4. Simulation drain–source voltages (V_{DS}) versus drain–source current (I_{DS}) of (a) SHEMT and (b) DHEMT.

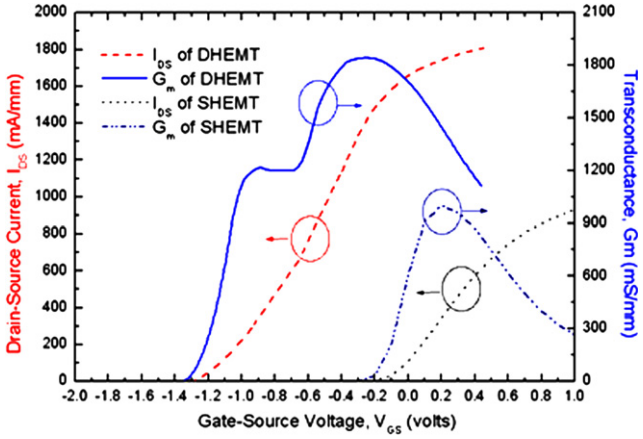

Fig. 5. Gate–source voltages (V_{GS}) versus drain–source current (I_{DS}) and transconductance (G_m) of SHEMT and DHEMT.

when T_1 and T_2 both are 25 nm, the channel is difficult to turn off. In addition, when T_1 is 25 nm and T_2 is 20 nm, larger voltage swing could be obtained. In addition, the threshold voltage is very sensitive to the sum of top and bottom barrier thicknesses ($T_1 + T_2$). When the total barrier thickness decreases, the absolute value of a threshold voltage decreases. Fig. 8 shows the variation of G_m under

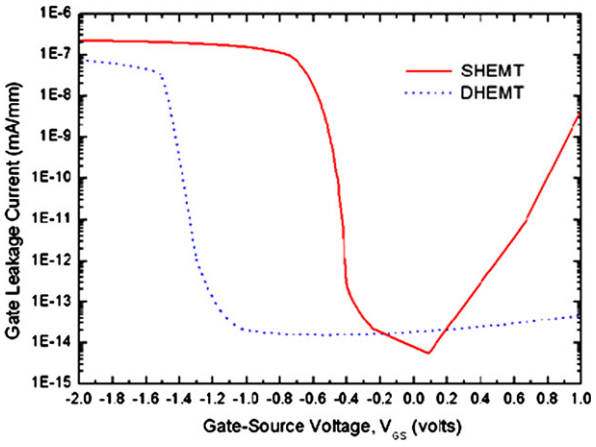

Fig. 6. The gate leakage current versus gate–source voltages (V_{GS}) of SHEMT and DHEMT.

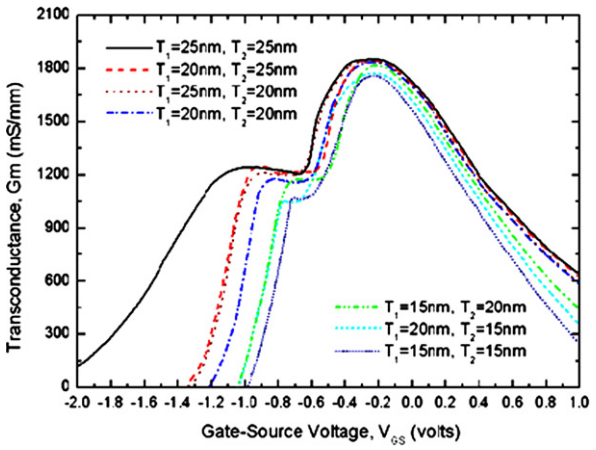

Fig. 7. Gate–source voltages (V_{GS}) versus transconductance (G_m) for various top barrier thickness (T_1) and bottom barrier thickness (T_2) of DHEMT.

different doping concentrations cases. Best voltage operation ranges of G_m can be obtained. It shows that the doping effect on the transconductance is dominant on the top δ-doped layer. However, the threshold voltage and gate operation reign are effected by bottom δ-doped layer dominantly.

The design criteria identifying the structure layer design for DHEMTs are expressed as follows:

1. The addition of the second channel in HEMT structure can improve the total channel carrier density, current driving capability and transconductance. Besides, it can keep a good pinch-off feature and reduce the leakage current.
2. Asymmetric dopant structure is suggested in DHEMT. Since the gate control is more sensitive on the top channel, proper asymmetry between two dopant layers can obtain a higher gain than a symmetric one. A higher doping concentration on top δ-doped layer is suggested.

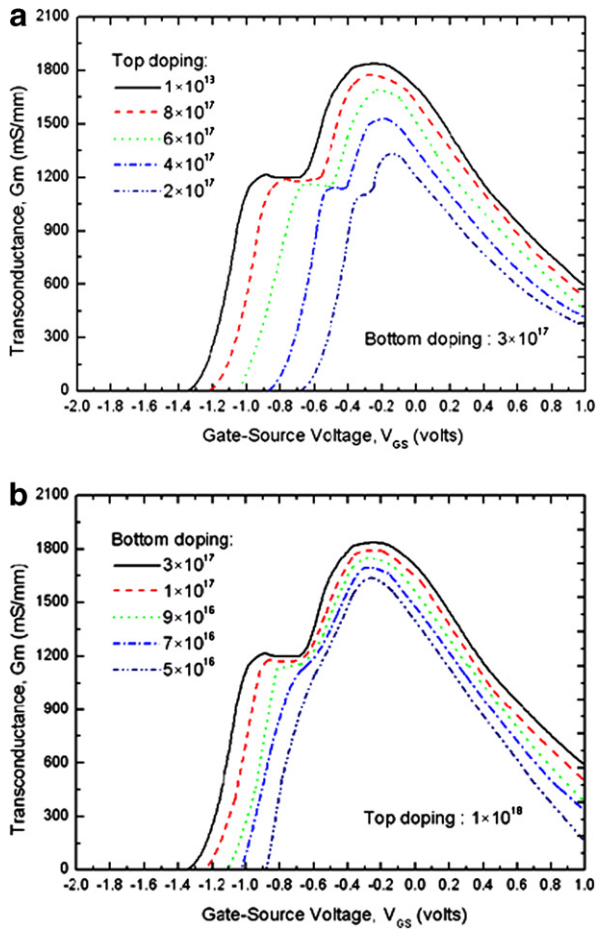

Fig. 8. Gate–source voltages (V_{GS}) versus transconductance (G_m) for various (a) top and (b) bottom δ-doped concentration of DHEMTs.

3. A higher doping concentration in δ-doped layer can enhance the transconductance.
4. The increase of barrier thickness can decrease the leakage current, and increase the turn-on voltage.
5. Thick spacer layer can reduce Coulomb scattering but reduce the current density.
6. Increasing the total thickness of superlattice layers in DHEMT would enhance the transconductance. However, the critical thickness for lattice matching should be concerned.

4. Conclusions

The design criteria of the DHEMTs are proposed in this paper. The InAlAs/InGaAs/InP DHEMTs are simulated and analyzed by MEDICI in which a self-consistently model based on the Poisson's and Schrödinger's equations are used. The results are also compared to that in SHEMT structure. Also, the relationship between the transconductance, the barrier thickness and the doping concentration are investigated. The results lead the conclusion that the doping concentration on the top δ-doped layer affects the G_m dominantly. When the doping concentration increases, the G_m increases. However, the threshold voltage and gate operation reign are effected by bottom δ-doped layer dominantly. When the doping concentration decreases, the absolute value of a threshold voltage decreases and the gate operation region becomes narrow. The leakage currents can be drastically reduced in DHEMT structure because of the effective double block from electron tunneling by the design of dual-channel (dual barrier) structure. The simulation results show that DHEMT structures have higher 2DEG density, higher sheet carrier density, high voltage swing, good carrier confinement, lower gate leakage current, high maximum drain–source current (up to 1425 mA/mm), and high transconductance (up to 1836 mS/mm). It is good for the high power device application.

References

[1] Kasemsuwan V. Circuits and systems, 1998. IEEE APCCAS 1998. The 1998 IEEE Asia-Pacific conference, November 24–27 1998. p. 783.
[2] Gupta Ritesh, Aggarwal Sandeep Kumar, Gupta Mridula, Gupta RS. Solid State Electron 2005;49:167.
[3] Chen Yeong Jia, Hsu Wei Chou, Chen Yen Wei, Lin Yu Shyan, Hsu Rong Tay, Wu Yue Huei. Solid State Electron 2005;49:163.
[4] Chen Yen Wei, Hsu Wei Chou, Hsu Rong Tay, Wu Yue Huei, Chen Yeong Jia. Solid State Electron 2004;48:119.
[5] Chihiro Hamaguchi, Kazuo Miyatsuji, Hiroki Hihara. Jpn J Appl Phys Part II Lett 1984;23:132.
[6] Sheng NH, Lee CP, Chen RT, Miller D L, Lee SJ. IEEE Electr Device Lett 1985;6:307.
[7] Tomizawa M, Furuta T, Yokoyama K, Yoshii A. IEEE Electr Device 1989;36:2380.
[8] Frank Schwierz, Liou Juin J. Modern microwave transistors: theory, design, and performance. A John Wiley & Sons; 2002.
[9] Liu Wen Chan, Chang Wen Lung, Lour Wen Shiung, Pan His Jen, Wang Wei Chou, Chen Jing Yuh, et al. IEEE Electr Device Lett 1999;20:548.
[10] Geiger D, Dickmann J, Wölk C, Kohn E. IEEE Electr Device Lett 1995;16:30.
[11] Thomas Kerkhoven, Raschke Michael W, Umberto Ravaioli. J Appl Phys 1993;74:1199.
[12] Li AZ, Chen YQ, Chen JX, Qi M, Liu XC, Chen J, et al. J Cryst Growth 2003;251:816.
[13] Taurus – Medici™ User Guide Version V-2003.12, 2003: 2–121.
[14] Lui WW, Fukuma M. J Appl Phys 1986;60:1555.
[15] Ladner C, Berthelemot-Aupetit C, Decobert J, Harmand JC, Post G, Vigier P, et al. Indium phosphide and related materials, In: 1998 International Conference, 1998. p. 505.
[16] Maher H, Decobert J, Falcou A, Le Pallec M, Post G, Nissim YI, et al. IEEE Electr Device 1999;46:32.